

## An Efficient Fluoride Ions Removal from Groundwater by Carbon Alumina Composites Materials

K. PREMALATHA<sup>1</sup>, B. PADMA<sup>2</sup> and V. SHASHIKALA<sup>1,\*</sup>

<sup>1</sup>Department of Chemistry, University College for Women, Osmania University, Hyderabad-500095, India

<sup>2</sup>Department of Chemistry, University Post Graduate College, Osmania University, Secunderabad-500003, India

\*Corresponding author: E-mail: shashikala\_chem@osmania.ac.in

Received: 6 June 2022;

Accepted: 28 July 2022;

Published online: 19 September 2022;

AJC-20976

Due to toxicity, persistent nature, bioaccumulation of fluoride ions and its alarming rise in different parts of India, it has become of utmost importance for the synthesis of an efficient material to remove fluoride ions from groundwater. This article reports the synthesis of highly efficient defluoridation carbon and alumina composite materials (CACM). A series of six samples were synthesized by deposition precipitation method and characterized using various techniques like XRD, BET surface area, pore size distribution, FT-IR, CO<sub>2</sub> chemisorption and CO<sub>2</sub> temperature programmed desorption (TPD) studies. Their efficiency of defluoridation activity was evaluated and observed that CACM 25 adsorbent exhibited excellent defluoridation activity of 98%.

**Keywords:** Defluoridation, Adsorbents, Carbon alumina composite Materials, Activity evolution.

### INTRODUCTION

Fluoride is an essential trace element for healthy dental and skeletal growth. However, an excess intake of fluoride into body can cause serious health disorders like osteoporosis, arthritis, hip fracture, cancer, Alzheimer's, brain damage, thyroid disorder, etc. [1-7]. Atmospheric air also contains fluoride as hydrogen fluoride, hydrofluoric acid, etc. Dhaka *et al.* [8] clearly explained about the fluoride mineral belts and the countries get affected by fluoride on the earth. Baba & Tayfur [9] discussed various geological processes, like water-rock interactions, tectonic processes, weathering, etc. of fluoride leaching from mineral rocks to the ground water. Fluoride can also accumulate in food from industrial effluents, moreover, atmospheric fluoride deposition is found on the food grown in fields [10,11].

Sometimes for strength of bone and teeth, fluorosilicic acid, sodium hexafluorosilicate and sodium fluoride were used in the municipal water fluoridation schemes [12,13]. Among all sources drinking ground water is the main source of fluoride entering in the body. According to WHO in 1996 limitations, fluoride concentration must be in the range of 1.0-1.5 ppm, whereas The Bureau of Indian Standards (BIS) sets a limit of 1 mg/L [14] while the Council of Medical Research of India [15] defines 1.5 mg/L as the safety limit. At the same time as

groundwater is widely distributed, despite of its high fluoride content, all over the world more than 260 million people consume drinking water with a fluoride concentration higher than 1.0 mg/L. Majority of these people live in tropical regions, 14 countries in Africa, eight in Asia and six in the Americas (UNICEF's Position on Water Fluoridation 2014), and many of them are confronted with problems due to endemic fluorosis, either dental or skeletal. Thus, it has become an utmost important for the synthesis of an efficient material to remove fluoride from ground water. This article reports about the synthesis of highly efficient carbon and alumina composite materials (CACM) for the defluoridation activity. A series of six samples were synthesized by deposition precipitation method and were characterized using various techniques like XRD, BET surface area, pore size distribution, FT-IR, CO<sub>2</sub> chemisorption and CO<sub>2</sub> temperature programmed desorption (TPD) studies. Their efficiency of defluoridation activity was evaluated and observed that sample CACM-25 adsorbent exhibited an excellent defluoridation activity.

### EXPERIMENTAL

**Preparation of carbon alumina composite materials (CACM):** Defluoridation activity of carbon alumina composite

materials (CACM) were compared with commercially available Active Carbon (C) and  $\text{Al}_2\text{O}_3$  (A) purchased from company Loba Chemie, India were used as such. A series of six CACM adsorbents with carbon weight percentage 5, 10, 15, 20, 25 and 50 were prepared by deposition precipitation method [16]. According to them six batches of adsorbents were prepared. Requisite amount of aluminium nitrates, purchased from Loba Chemie India, were dissolved in distilled water to prepare a 5% precursor solution then 5, 10, 15, 20, 25 and 50 wt.% of finely powdered active carbon were added in batchwise. The precursor solution along with powdered active carbon taken in a beaker were precipitated with 5% aqueous  $\text{NH}_3$  solution by adding dropwise with continuous stirring. Thus, formed gelatinous white precipitate was filtered and washed with distilled water to a pH 7. Then, the filtered sample cakes were oven dried at 120 °C for overnight and calcined at 350 °C in inert atmosphere for 3 h. These adsorbents after activation are activated by soaking in 3 % aluminium sulphate solution for 1 h followed by decantation. Then the adsorbents were washed thoroughly with deionized water till the decant solution become neutral pH. Then these adsorbents were kept for drying in oven at 120 °C for 4 h.

**Characterization:** All the adsorbent materials *viz.* CACM-5, CACM-10, CACM-15, CACM-20, CACM-25 and CACM-50 were characterized using different techniques like XRD,  $\text{N}_2$ -adsorption desorption, FT-IR and  $\text{CO}_2$  chemisorption and temperature programmed desorption studies.

The XRD patterns of adsorbents were recorded on a Rigaku Miniflex X-ray diffractometer (Rigaku Corporation, Japan) using Ni filtered  $\text{CuK}\alpha$  radiation adjusting  $2\theta$  ranging  $2^\circ$  to  $80^\circ$  and with  $2\theta$  scan speed of  $2^\circ/\text{min}$ . BET-surface areas of the adsorbents were measured on an all glass high vacuum system by  $\text{N}_2$  adsorption at  $10^{-6}$  torr vacuum at  $-196^\circ\text{C}$ . Pore size distribution of best adsorbent CACM-25 was calculated by BJH method with the help of Autosorb-1 Gas adsorption system (Quantachrome Instruments, USA). FT-IR spectrum is recorded between wave length range of  $4000\text{--}400\text{ cm}^{-1}$  on FT-IR spectrophotometer Spectrum GX (Perkin-Elmer, USA). In a typical experiment, about 100 mg of adsorbents are placed in a glass micro reactor and pretreated at 673 K for 1 h under He flow. After the pretreatment, the adsorbents were allowed to cool to 333 K. Then 10%  $\text{CO}_2$  in He mixture gas was injected in pulses through a 500  $\mu\text{L}$  loop connected to the six-port valve until no further change in the intensity of the outlet  $\text{CO}_2$  was observed. After the completion of the pulse chemisorptions, temperature programmed desorption of adsorbed  $\text{CO}_2$  gas was performed. In this process the reactor temperature was increased linearly at a programming rate of 10 K/min from room temperature to 1073 K where 30 min isothermal conditions were maintained followed by cooling to room temperature. The patterns were monitored through a computer workstation equipped with CLASS GC-10 software package to process the signal coming out of TCD. This configuration allows finding out amount and nature of  $\text{CO}_2$  adsorbed on the catalyst.

**Activity evaluation:** Each adsorbent (1 g) was taken in the vertical glass reactor sandwiched between the cotton plugs,

and then fluoride containing water was passed through the catalyst in different flow rates with the help of a feed pump. Fluoride ions present in the water collected in the outlet was analyzed in advanced ion chromatography (Metrohm Limited, Switzerland) associated with a conductivity detector. Out let sample of 20  $\mu\text{L}$  was injected through the column METROSEP A Supp 100/4.0. Eluent used for the analysis of fluoride ion was a mixer solution of 3.2 mM  $\text{Na}_2\text{CO}_3$  + 1.0 mM  $\text{NaHCO}_3$  and the flow rate was kept as 0.7 mL/min.

## RESULTS AND DISCUSSION

**XRD studies:** XRD patterns of series of adsorbent material from CACM 5 to CACM 50 after treating with aluminium sulphate solution are shown in Fig. 1. With increase in the carbon percentage of the adsorbents, a clear phase transformation from boehmite with  $d$ -values 1.86 ( $2\theta = 49.2^\circ$ ), 3.17 ( $2\theta = 28.12^\circ$ ), 6.15 ( $2\theta = 14.07^\circ$ ) (ICDD file no.: 01-1283) to  $\gamma$ -alumina with  $d$ -values 1.4 ( $2\theta = 66.8^\circ$ ) 1.98 ( $2\theta = 45.5^\circ$ ), 2.39 ( $2\theta = 36.9^\circ$ ) (ICDD file no.: 01-1303) was observed. This may be due to the reason that as the carbon percentage increases in adsorbents; the alumina might have dispersed finely on the carbon in deposition-precipitation method. And under mild calcination conditions (623 K/3h), highly dispersed particles of aluminium hydroxide particles on carbon generated aluminium oxide hydroxide (boehmite) with low carbon weight percentages and with high weight percentages could generate  $\gamma\text{-Al}_2\text{O}_3$  phase with more dispersion in CACM adsorbents.

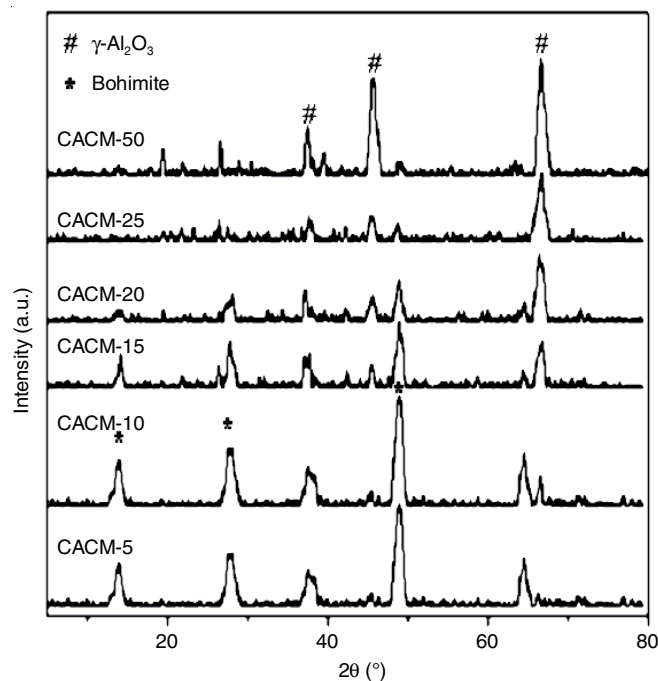


Fig. 1. XRD patterns of CACM adsorbents before activation

Ratios of  $\gamma$ -alumina, boehmite phases and their crystallite sizes present in all the CACM adsorbents are given in Table-1. It is observed that  $\gamma$ -alumina phase was increased at the expense of boehmite phase against carbon loading (from CACM 5 to CACM 50). Particle size of boehmite was decreased and that

TABLE-1  
RATIO OF CRYSTALLINE PHASES AND SIZES OF  
 $\gamma$ -ALUMINA:BOHMITTE PHASES OF CARBON  
ALUMINA COMPOSITE MATERIALS

| Adsorbent | Crystallite size (nm)                                 | Ratio of phases (%)                                   |
|-----------|---|---|
|           | = $\gamma$ -Al <sub>2</sub> O <sub>3</sub><br>Bohmite | = $\gamma$ -Al <sub>2</sub> O <sub>3</sub><br>Bohmite |
| CACM-50   | 123/-   | 0.86  |
| CACM-25   | 83/-  | 0.95  |
| CACM-20   | 64/-  | 1.03  |
| CACM-15   | 35/54   | 1.15  |
| CACM-10   | -/74  | 2.62  |
| CACM-5    | -/76  | 2.10  |

Note: Crystallite size was calculated from XLB method

of  $\gamma$ -alumina was increased against the carbon loading. These results clearly stated that fine dispersion of aluminium hydroxide phase on finely powdered carbon could transform to  $\gamma$ -alumina phase even at mild calcination conditions [17].

**BET and pore size distribution:** Surface area values of six adsorbents CACM prepared by deposition precipitation method obtained experimentally were compared with the theoretical values of surface area of samples prepared by physical mixing [9]. A distinguishable large difference in the surface area values of these two sets of adsorbents was clearly evident from Fig. 2. In both the cases, the surface area values were increased with increase in the weight percent of carbon. However, high increase in the surface area of the samples prepared by deposition precipitation of alumina on powdered carbon might be due to dispersive deposition-precipitation of aluminium hydroxide by dilute ammonia solution on to the high surface area carbon.

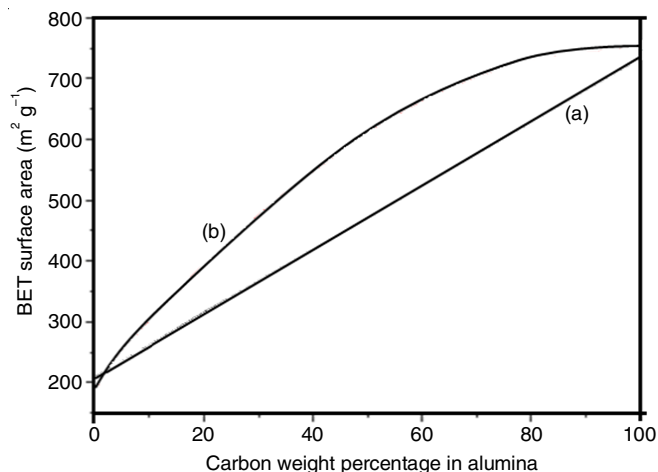


Fig. 2. BET-SA of carbon alumina composite materials (a) physical mixing of carbon and alumina (b) deposition precipitation of alumina on carbon

Pore size distribution of as-purchased carbon,  $\gamma$ -alumina and best adsorbent among the prepared carbon alumina composite materials, CACM-25 is given in Fig. 3. According to the literature [17-20], types of pores present in carbon and alumina possess both micro and mesopores. Fig. 3 clearly shows the presence of bimodal pores *i.e.* micro (< 20 Å) and meso (~ 50 Å) pores on carbon and mesopores on alumina (between

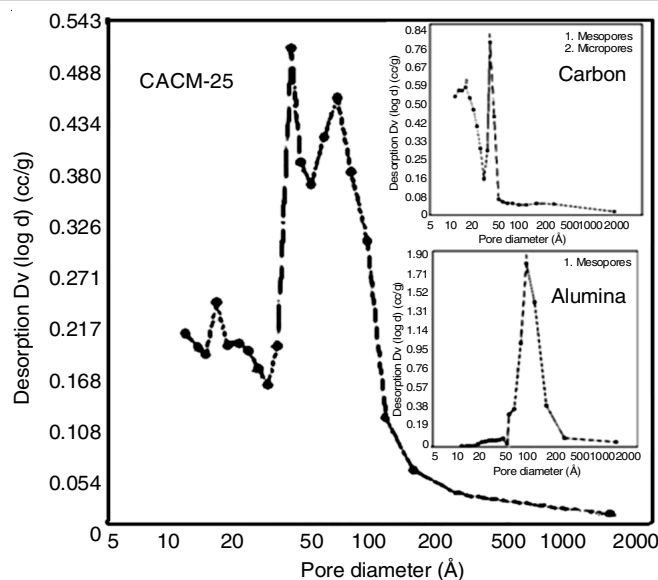


Fig. 3. Pore size distribution of carbon, alumina, CACM-25

50-250 Å). Combination of pore size distribution pattern of both carbon and alumina can be seen in CACM-25. Pore size distribution in case of carbon is also with bimodal pores (micro and mesopore), but major contribution is from micropores. Alumina contains only mesopores in the range 50-150 Å. CACM-25 prepared by precipitating alumina over powdered carbon has acquired both pore structures of alumina and carbon.

**FT-IR studies:** A strong, broad peak in the range of 3600-3400 cm<sup>-1</sup> attributed to O-H stretching vibration of water, which is associated with the samples, are unambiguously seen in all the samples (Fig. 4). A band ~1600 cm<sup>-1</sup> observed in CACM-25 has been attributed to the H<sub>2</sub>O bending vibrations with its intensity being dependent on the amount of water present in the interlayers [21]. The other bands seen in the region 1000-400 cm<sup>-1</sup> can be related to various stretching and bending vibrations of Al-O and Al-O bonds [22]. The peak around 1200-1000 cm<sup>-1</sup> and a strong peak corresponding to  $\nu_{s=0}$  stretching vibrations of surface sulphate groups ~1400 cm<sup>-1</sup> were observed in all the adsorbents. Nakamoto *et al.* [23] reported that bidentate sulphate groups show distinct peaks in the region 1400-950 cm<sup>-1</sup> with a strong peak at 1386 cm<sup>-1</sup> corresponding to  $\nu_{s=0}$  stretching vibrations of surface sulphate groups. Intensity for the sulphate peaks were increased with decreasing the alumina weight percentage. This may be due to the reason that with increasing carbon percentage alumina is in more dispersed form and the number of OH<sup>-</sup> groups available for exchanging with sulphate is also increasing. Maybe the number of sulphate groups on CACM-25 are sufficient for removing fluoride ions from water, this may be the reason for higher defluoridation activity of CACM-25 adsorbent.

**CO<sub>2</sub> chemisorption and TPD:** CO<sub>2</sub> uptake values for the alumina, carbon and CACM adsorbents were determined by pulse chemisorption technique. The amount of CO<sub>2</sub> uptake values are in relation with the defluoridation activities (Fig. 5). Adsorbent CACM-25 exhibited highest CO<sub>2</sub> uptake, which implies that this adsorbent possesses highest number of basic sites *i.e.* OH<sup>-</sup> exchangeable with F<sup>-</sup> ions.

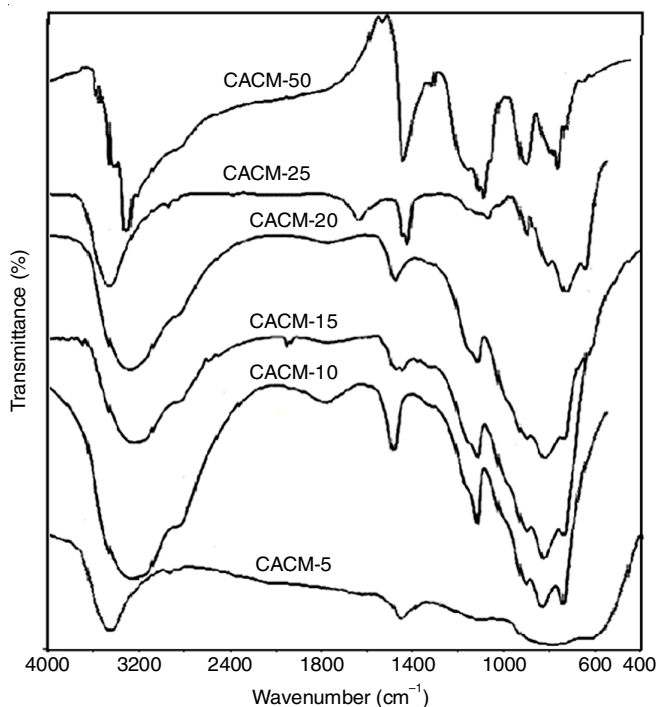


Fig. 4. FT IR spectra of activated CSAAs samples

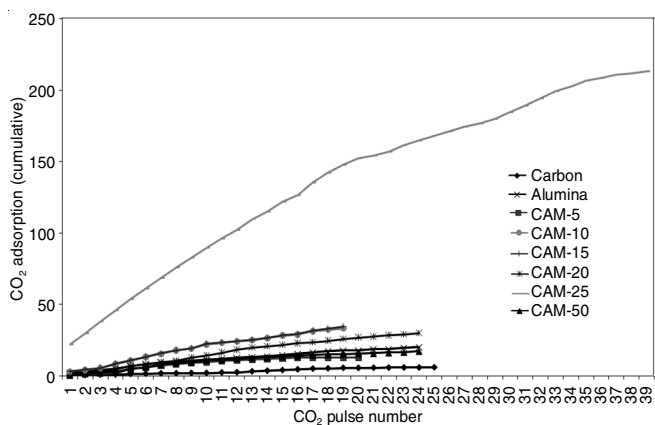


Fig. 5. CO<sub>2</sub> uptake on carbon, alumina and carbon alumina composite materials

Temperature programmed desorption (TPD) of CO<sub>2</sub> has been carried out for all the prepared CACM adsorbents. From Fig. 6, it can be clearly seen that all the adsorbents clearly show low temperature and high temperature peaks. In the lower loadings of carbon, three signals were observed *i.e.* a lower temperature signal at  $T_{max} \sim 260$  K, which corresponds to weak basic sites, next signal at  $T_{max} \sim 500$  K corresponds to the moderate basic sites and the third signal at  $T_{max} \sim 650$  K is attributed due to the strong basic sites [24]. As carbon loading increases signal for moderate basic sites collapses and a broad signal of strong basic sites emerges.

**Activity evaluation:** All the prepared adsorbents were tested for their defluoridation capacity. Each adsorbent (1 g) was finely sieved and taken in a glass reactor of 12 mm internal diameter and 20 ppm fluoridated water was passed over the adsorbents in a continuous flow method. Fluoride ions present in the out let water was collected analyzed for fluoride ions

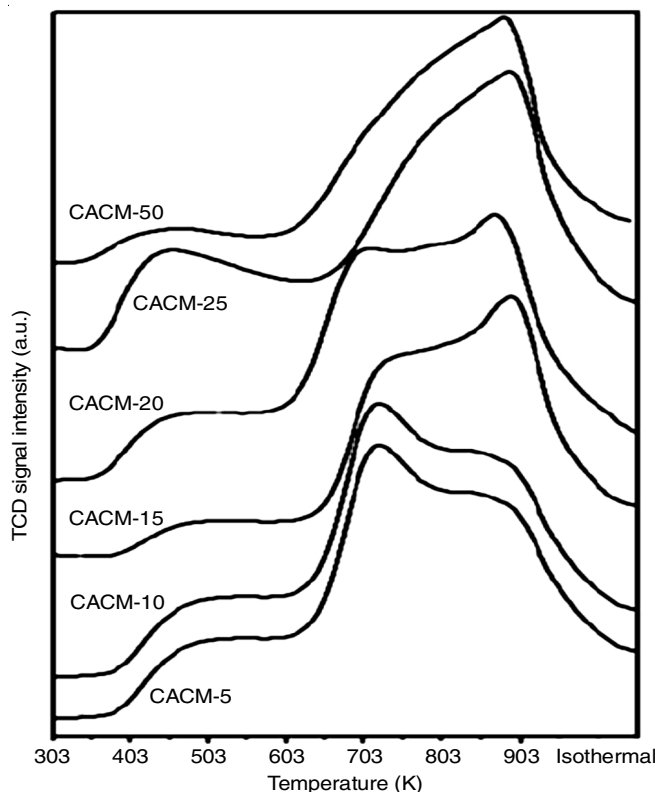


Fig. 6. CO<sub>2</sub> TPD patterns of CACM adsorbents

with the help of advanced ion chromatograph mobile phase, which consist of the mixture (Na<sub>2</sub>CO<sub>3</sub> + NaHCO<sub>3</sub>) solution in deionized water.

Fig. 7 shows the percent adsorption capacity of all the adsorbents and the weight percentage of carbon present in the adsorbents. These results indicated that among all adsorbents CACM with carbon 25 wt.% exhibited higher defluoridation activity, which removes fluoride almost 98%. Fluoride adsorption capacity of CACM-25 was tested with different flow rates rates like 10, 20, 30, 60 and 100 mL/h on the defluoridation capacity of all the prepared adsorbents. Their defluoridation capacities measured at 5 h are given below in Table-2. It was observed that there was decrease in the strength of the

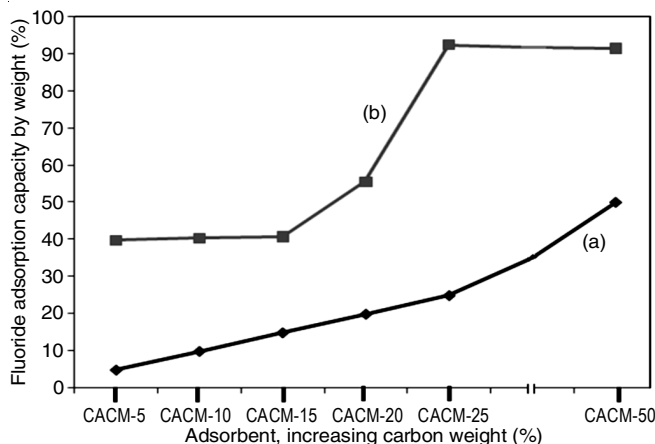


Fig. 7. Defluoridation capacity of CACM adsorbents (a) carbon weight percentage and (b) defluoridation capacity

| Adsorbents | F adsorption capacity (by wt %) cumulative value at 5 h |         |         |         |          |
|------------|---|---------|---------|---------|----------|
|            | 10 mL/h   | 20 mL/h | 30 mL/h | 60 mL/h | 100 mL/h |
| CACM-5     | 42  | 42      | 40      | 34      | 30       |
| CACM-10    | 44  | 42      | 40      | 36      | 32       |
| CACM-15    | 44  | 43      | 41      | 36      | 32       |
| CACM-20    | 62  | 60      | 55      | 47      | 40       |
| CACM-25    | 99  | 98      | 98      | 86      | 52       |
| CACM-50    | 91  | 91      | 91      | –       | –        |

sieved pellets in case of CACM-50, thus there is obstruction in the flow of water through this sample. From third hour onwards, pellet sieves have starting collapsing at higher flow rates that is 60 and 100 mL/h. Fluoride adsorption capacity by weight percent on carbon was 26.8 mg/g and on commercial alumina it was 48.6 mg/g.

**Effect of flow rate:** As shown in Table-2, there was a decrease in the fluoride adsorption capacity with increase in the flow rates. Among all the prepared adsorbents, CACM 25 exhibited excellent adsorption capacity 99%, 98%, 98%, 86% and 52% adsorption at 10, 20, 30, 60 and 100 mL/h flow rates, respectively. High rate of flow and high fluoride adsorption are advisable for practical application purposes. Thus, flow rate of 30 mL/h has been taken for time on stream study on CACM-25 adsorbent. Fig. 8 represents the percent adsorption capacity of adsorbent with time and cumulative weight of fluoride adsorbed in milligram of fluoride per one gram of adsorbent per time of 26 h.

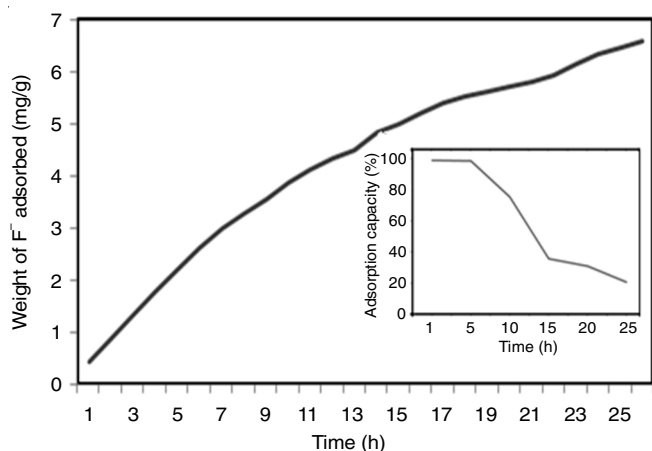


Fig. 8. Time on stream studies over CACM-25 adsorbent with 30 mL/h flow rate

## Conclusion

After studying the defluoridation properties of commercially available carbon and alumina, best adsorption properties of these materials were incorporated in the synthesis of an efficient defluoridation adsorbent carbon alumina composite material. The defluoridation activity is almost constant in the CACM adsorbents with carbon loadings from 5 to 15 and the adsorption capacity was increased and reaches maximum 91 % with carbon 25 wt.% and then decreased. The defluoridation activities were comparable with the CO<sub>2</sub> pulse chemisorptions

results. BET surface area values of the carbon-alumina composite materials were also increased with increase in the carbon weight percentage upto 25%. From the CO<sub>2</sub> TPD results, it was observed that with increase in the carbon percentage the moderate basic sites were transformed to strong basic sites. FTIR studies revealed that the more number of exchangeable OH/SO<sub>4</sub><sup>2-</sup> were observed in CACM-25. From the flow rate experiments and time on stream studied, it was known that CACM-25 has the highest mechanical strength too and also exhibited an efficient removal of fluoride not only with lower flow rate of 30 mL/h/g cat. but also can work well upto 100 mL/h/g cat. This catalyst showed the defluoridation activity even after 25 h of continuous contact with the fluoridated water. This property can be considered highly in the preparation of large scale purposes for practical applications.

## CONFLICT OF INTEREST

The authors declare that there is no conflict of interests regarding the publication of this article.

## REFERENCES

- S.J. Kashyap, R. Sankannavar and G.M. Madhu, *J. Hazard. Mater. Lett.*, **2**, 100033 (2021); <https://doi.org/10.1016/j.hazl.2021.100033>
- R. Ullah, M.S. Zafar and N. Shahani, *Iran. J. Basic Med. Sci.*, **20**, 841 (2017); <https://doi.org/10.22038/IJBMS.2017.9104>
- M.S. Kurdi, *Indian J. Anaesth.*, **60**, 157 (2016); <https://doi.org/10.4103/0019-5049.177867>
- E.A. Martínez-Mier, *J. Evid. Based Complem. Altern. Med.*, **17**, 28 (2011); <https://doi.org/10.1177/2156587211428076>
- D. Kanduti, P. Sterbenk and B. Artnik, *Mater. Sociomed.*, **28**, 133 (2016); <https://doi.org/10.5455/msm.2016.28.133-137>
- S. Dey and B. Giri, *Med. Clin. Rev.*, **2**, 1 (2016); <https://doi.org/10.21767/2471-299X.1000011>
- P. Grandjean, *Environ. Health*, **18**, 110 (2019); <https://doi.org/10.1186/s12940-019-0551-x>
- A. Chowdhury, M.K. Adak, A. Mukherjee, P. Dhaka, J. Khatun and D. Dhaka, *J. Hydrol.*, **574**, 333 (2019); <https://doi.org/10.1016/j.jhydrol.2019.04.033>
- A. Baba and G. Tayfur, *Environ. Monit. Assess.*, **183**, 77 (2011); <https://doi.org/10.1007/s10661-011-1907-z>
- M. Vithanage and P. Bhattacharya, *Environ. Chem. Lett.*, **13**, 131 (2015); <https://doi.org/10.1007/s10311-015-0496-4>
- M. Habuda-Stanic, M. Ravančić and A. Flanagan, *Materials*, **7**, 6317 (2014); <https://doi.org/10.3390/ma7096317>
- R.N.V. Rao, N. Rao and R.D. Schuiling, *Environ. Geosci.*, **21**, 84 (1993).
- G. Ateria, V.K. Khadder and S. Phadnis, *Int. J. Theor. Appl. Sci.*, **7**, 21 (2015).
- Draft Indian Standard DRINKING WATER – SPECIFICATION, (Second Revision of IS 10500), ICS No. 13.060.20; Report of Bureau of Indian Standards Doc, FAD, **25**, C (2009).
- Special Report, The Indian Council of Medical Research. New Delhi: National Institute of Science Communication, Indian Science Congress, Food Nutrition and Environment Security. The Road Ahead, vol. series 44 (1975).
- K.S. Rama Rao, V. Shashikala, A.H. Padmasri, B.D. Raju, V.S. Kumar, B.M. Nagaraja, P. Seetharamulu, S.S. Reddy, U.C. Kulshreshtha and K.V.R. Chary, A Process for the Preparation of Highly Efficient Carbon Supported Activated Alumina Adsorbent for Removal of Fluoride Ion from Water, US Patent 2006254989(A1) (2006).

17. P. Palmero, B. Bonelli, F. Lomello, E. Garrone and L. Montanaro, *J. Therm. Anal. Calorim.*, **97**, 223 (2009); <https://doi.org/10.1007/s10973-009-0260-8>
18. R.C. Bansal, J.B. Donnet and F. Stoeckli, *Active Carbon*, Marcel Dekker: New York (1988).
19. H. Marsh and F. Rodriguez-Reinoso, *Activated Carbon*, Elsevier: Amsterdam (2006).
20. A. Goswami and M.K. Purkait, *Chem. Eng. Res. Design*, **90**, 2316 (2012); <https://doi.org/10.1016/j.cherd.2012.05.002>
21. S. Miyata, *Clays Clay Miner.*, **23**, 369 (1975); <https://doi.org/10.1346/CCMN.1975.0230508>
22. D. Tichit, M.H. Lhouty, A. Guida, B.H. Chiche, F. Figueras, A. Auroux, D. Bartalini and E. Garrone, *J. Catal.*, **151**, 50 (1995); <https://doi.org/10.1006/jcat.1995.1007>
23. K. Nakamoto, J. Fujita, S. Tanaka and M. Kobayashi, *J. Am. Chem. Soc.*, **79**, 4904 (1957); <https://doi.org/10.1021/ja01575a020>
24. V. Siva Kumar, B.M. Nagaraja, V. Shashikala, P.S. Ramulu, A.H. Padmasri, B.D. Raju and K.S. Rama Rao, *J. Mol. Catal. A. Chem.*, **223**, 283 (2004); <https://doi.org/10.1016/j.molcata.2003.08.034>